Fatigue Analysis of a Commercial Vehicle Axle Body using the Short Crack Model

G. Savaidis
Department of Mechanical Engineering, Aristotle University of Thessaloniki, 54124 Thessaloniki, Greece

ABSRACT

Using a commercial vehicle forged axle body made of a low-alloyed steel as an example, the present paper demonstrates the usefulness of the Short-Crack-Model for the fatigue analysis and the design optimization of engineering components during their early developmental stage. The cyclic material input data used were approximated by means of the Uniform Material Law based only on monotonic material properties. The design load sequences acting at the axle have been measured during driving a vehicle on an appropriate test track. The influence of the surface roughness has been evaluated using the equation of Hück et al.. Life reducing effects resulting from the variable amplitude loading sequence have been explored comparing SCM-calculations with conventional ones based on the P_{SWT}-parameter. The main task of the investigation is the evaluation of stress ratios of real acting to allowable maximum stresses at the failure-critical locations of the axle body, which quantify the necessity for local design optimization to achieve satisfactory fatigue lifetime.

1 INTRODUCTION

In view of the increasing demand to reduce developing times and costs of novel engineering products, computational models for fatigue analysis become more and more important even in the hitherto more experimentally oriented application areas. Among many models available in the literature, the Short-Crack-Model (SCM) developed by Vormwald [1] based on fracture mechanics analysis of semi-circular surface micro-cracks offers one possible way to predict fatigue life-to-initiation of cracks with lengths of technical size (≈1mm) in structural components under variable amplitude loading.

This paper shows the fatigue analysis performed in accordance with the SCM to optimize the local design of a forged commercial vehicle axle body at an early stage of development, when prototype components are not available. Emphasis is given on the elastic-plastic analysis considering the influences from the surface roughness and the variable amplitude load sequence.

2 DESCRIPTION OF THE SHORT-CRACK-MODEL

The SCM assumes that there is either a pre-existing micro-crack at the failure-critical point of the component under investigation or the lifetime to the initiation of the micro-crack under cyclic loading is very short. The growth of such micro-cracks of a certain crack-depth a_0 to a final (failure) crack-depth a_f of about 1 mm is described by elastic-plastic fracture mechanics. The input data of the model are:

- the crack-growth law ($da/dn=f(\Delta J_{eff})$), the cyclic stress-strain curve ($\varepsilon_a=f_1(\sigma_a)$) and the constant amplitude strain-life curve ($\varepsilon_a=f_2(N)$) of the material,
- the elastic notch factor c^*, expressing the relation between elastic local strain ε_{el} and external load L
- the load sequence.

Taking the material data as a basis, the macroscopic elastic-plastic σ-ε path at the failure location of the component is evaluated using c^*, a notch approximation formula such as the Neuber's rule [2], considering the Masing [3] and memory behavior. The effective ranges of stress $\Delta\sigma_{eff}$ and strain $\Delta\varepsilon_{eff}$ can be estimated using Newman's [4] crack opening stress equation developed for constant amplitude loading considering that crack opening and closure occur at nearly the same strain value [1].

Using the effective range of the J-integral ΔJ_{eff} as formulated by Dowling [5] and defining a crack-depth independent damage parameter P_J as

$$P_J = \frac{\Delta J_{eff}}{a} = 1{,}24 \cdot \frac{\Delta\sigma_{eff}^{\,2}}{E} + \frac{1{,}02}{\sqrt{n'}} \cdot \Delta\sigma_{eff} \cdot \left[\Delta\varepsilon_{eff} - \frac{\Delta\sigma_{eff}}{E} \right], \tag{1}$$

lifetime-to-crack initiation (crack length≈1 mm) can be calculated using a linear damage accumulation theory. In eqn. (1) E and n' represent the Young's modulus and the cyclic hardening exponent of the material, respectively. For arbitrary load sequences, the integration of the crack-growth law is equivalent to the linear damage accumulation using a P_J-N-curve according to

$$P_J^m \cdot N = Q \qquad \text{for } P_J > P_{J,E} \qquad (P_{J,E} = \text{endurance limit in } P_J \text{ values}), \tag{2}$$

if a log-log representation for both the crack-growth rate curve and the P_J-N-curve is applied. The constant Q in eqn. (2) corresponds to the fatigue life at P_J=1 N/mm^2. The slopes of the crack-growth rate curve and the P_J-N-curve must have the same value m.

To consider the mutual effects between small and large cycles in the case of variable amplitude loading, Vormwald et al. [1] introduced additional algorithms for calculating the crack-opening strains on a cycle-by-cycle basis.

2.1. Consideration of the surface roughness

The best way to consider the surface condition is to determine the cyclic material properties using specimens, which exhibit the same surface conditions as the component under investigation. However, this way often requires a high precision manufacturing input and costs, and is, therefore, not feasible to many engineering applications. The most reasonable way is to use material data determined from polished specimens and to consider the influence of surface roughness separately.

Based on comprehensive experimental data from Lehr [6] and Siebel and Gaier [7], Hück et al. [8] proposed the following empirical approximate relationship to estimate the decrease of the stress endurance limit σ_E due to the surface roughness

$$\kappa = \frac{\sigma_{E,rough}}{\sigma_{E,pol}} = 1 - 0.22 \cdot \left(\log R_z\right)^{0.64} \cdot \log \sigma_{UTS} + 0.45 \cdot \left(\log R_z\right)^{0.53}. \tag{3}$$

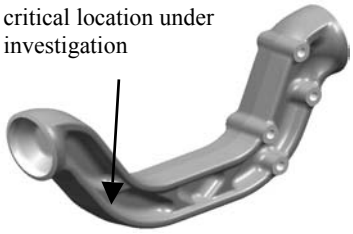

Figure 1: Axle body and critical location under investigation

The subscript "*E"* in eqn. (3) denotes the endurance limit. σ_{UTS} and the mean roughness R_z are to be substituted in N/mm^2 and µm, respectively.

Assuming that the elastic behavior is macroscopically dominant in the region of the endurance limit, the elastic term of eqn. (1) yields an approximation for the $P_{J,E}$-value to the rough surface condition

$$P_{J,E,rough} \approx 1{,}24 \frac{(\Delta\sigma_{eff})^2_{E,rough}}{E} = 1{,}24 \frac{(\kappa \cdot \sigma_{E,pol} - \sigma_{E,cl,rough})^2}{E}. \quad (4)$$

Herein, the crack closure stress $\sigma_{E,cl,rough}$ can be evaluated using Newman's [4] equations for a fully reversed stabilized σ–ε hysteresis with a stress amplitude of $\kappa \cdot \sigma_{pol}$.

As an approximation, the number of the failure cycles N and the slope m of the P_J-N curve describing the lifetime-limited path are assumed to be the same for the rough surface as that for the polished surface.

3 FATIGUE ANALYSIS OF THE AXLE BODY

Figure 1 shows a rough drawing of the forged axle body under investigation. Its nominal payload amounts to 83 kN. Several critical locations exist for which fatigue analyses have been performed. The arrow in Figure 1 indicates the most critical location for which the fatigue analysis and the corresponding results are presented in this paper.

3.1. Material properties

The axle is made of the fine-grained low-alloyed steel FeE500 produced in accordance with the German standard DIN 17103. At the time of this investigation, the required cyclic material data were neither available at the manufacturer of the axle nor in handbooks [9]. Therefore, they have been approximated by means of the Uniform Material Law (UML) [10]. The UML uses σ_{UTS} and E to estimate the material constants to describe the cyclic σ_a-ε_a curve in accordance with the Ramberg-Osgood Law [11]

$$\varepsilon_a = \frac{\sigma_a}{E} + \left(\frac{\sigma_a}{K'}\right)^{1/n'} \quad (5)$$

and the constant amplitude ε_a-N curve in accordance with Manson's [12] and Coffin's [13] equations

$$\varepsilon_a = \frac{\sigma_f'}{E}(2N)^b + \varepsilon_f'(2N)^c \quad (6)$$

Considering σ_{UTS} =610 N/mm^2 for FeE500 (according to DIN 17102) and E=210000 N/mm^2 for steel, the cyclic constants of FeE500 amount to:

$$K' = 1.65 \cdot \sigma_{UTS} = 1006\ N/mm^2, \quad (7)$$

$$n' = 0.15 \quad (8)$$

$$\sigma_f' = 1.5 \cdot \sigma_{UTS} = 915\ N/mm^2, \quad (9)$$

$$b = -0.087, \quad (10)$$

$$\varepsilon_f' = 0.5 \cdot \Psi = 0.5 \cdot 1 = 0.5 \qquad (\Psi = 1 \text{ for } \sigma_{UTS}/E \le 0.001). \quad (11)$$

$$c = -0.6 \quad (12)$$

3.2. Load sequences

The strain-time sequence acting at the critical location of the axle body has been measured by means of strain gages during test-driving on a test track using a *milled* axle providing the same dimensions as those of the forged axle under investigation. Figure 2 shows the two-dimensional level crossing spectrum derived from the measured strain-time sequence normalized by the maximum strain value ε_{max}.

3.3. Surface roughness

In accordance with the design instructions, the serial axle body will be manufactured by forging, and its surface will be cleaned by sand-peening after the forging process. As a result, roughness and residual stresses are expected to act at the surface.

Siebel and Gaier [7] designate possible mean roughness values R_z till up to 120 µm for a forged surface. Taking R_z=120 µm and σ_{UTS} =610 MPa into account, the κ-factor estimated with Hück's et al. [8] equation amounts to κ=0.69.

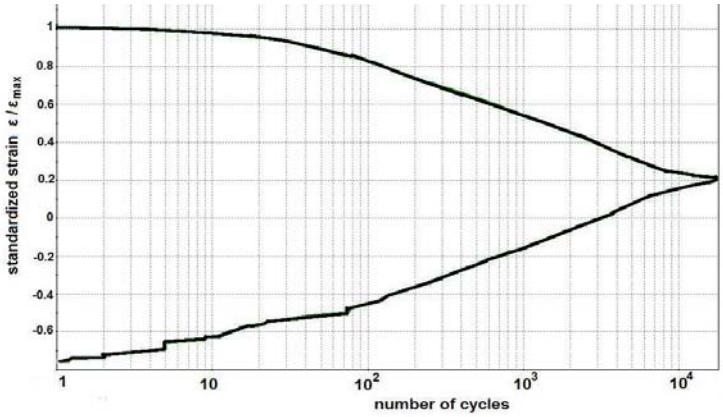

Figure 2. Normalized strain spectrum measured at the critical location

The shift of the P_J-N curve due to the surface roughness is calculated considering κ=0.69 and the endurance limit $P_{J,E,rough}$ according to eqn. (4) to

$$P_{J,E,rough} = 1{,}24\frac{(\kappa \cdot \sigma_{E,pol} - \sigma_{E,cl,rough})^2}{E} = 0.23\ . \tag{13}$$

Note that the values of R_z and σ_{UTS} used here are rough approximations and need to be experimentally verified as soon as a prototype axle is available.

3.4. Surface residual stress state

Residual stresses may arise to the surface due to the forging and the sand-peening processes. Using the example of a forged and sand-peened automotive steering shaft, Ref. [14] demonstrates that residual stresses have a secondary influence on the fatigue life compared to the one resulting from the surface roughness. They decrease rapidly when the surface of the component sees plastic deformations due to the external loading. In the present case study, the strains measured at the critical location point out significant local plastic deformations. Therefore, influence of residual stresses has not been considered in the current analysis.

Nevertheless, the residual stress state should be measured, e.g. by means of X-rays, when a prototype axle will be available, to adjust the theoretical analyses.

3.5. Results

Figure 3 shows the fatigue life results calculated in accordance with the SCM for the polished and rough surface condition and those calculated with the Local Strain Approach supported by the well-known parameter P_{SWT} of Smith-Watson and Topper [15]. The calculations concern the most critical location and are valid for P_S=50%.

Despite the fact that P_{SWT} generally disregards load sequence effects while SCM fully considers them, the comparison of both curves for the polished surface shows that these effects yield a factor of approximately 10 in the fatigue-life. The comparison of the SCM-curves for the polished and the rough surface condition explores a life factor of approximately 2 due to the rough-

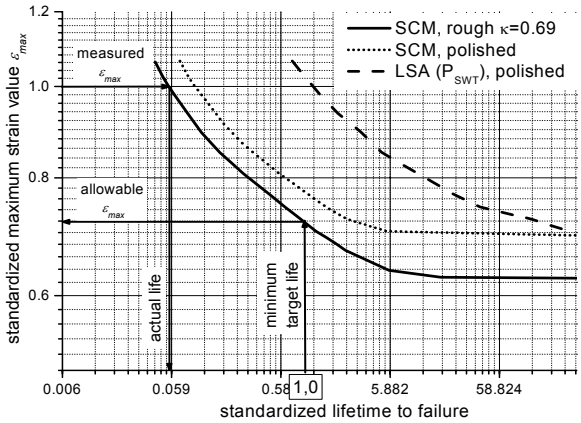

Figure 3: Fatigue life curves calculated in accordance with the SCM and the P_{SWT} parameter

ness influence. In accordance with the SCM-calculations the maximum stress has to be reduced to its allowable value of 72% of the actual one. The P_{SWT}-calculation would accept the actual axle design.

4 CONCLUSIONS

- When only monotonic material properties are available, the application of the UML is a practicable way to obtain the necessary cyclic input data. In this manner, the amount of experimental works required for determining cyclic material data can be considerably reduced.
- Effects resulting from the variable load sequence and the surface roughness can be reasonably considered and quantified within the SCM.
- The local design of the axle has to be optimized in a way that the maximum allowable strain will not exceed 72% of the measured value.

5 REFERENCES

1. Vormwald M, Seeger T. The consequences of short crack closure on fatigue crack growth under variable amplitude loading. Fat. Frac. Engng Mater. Struct.14(2/3), 205-225, 1991.
2. Neuber H. Theory of stress concentration for shear-strained prismatical bodies with arbitrary nonlinear stress-strain law. J. Appl. Mech. 12, 544-550, 1961.
3. Masing, G. Eigenspannungen und Verfestigung beim Messing. Proc. 2nd Int. Congress of Appl. Mech., 332-335, 1926.
4. Newman JC jr. A crack opening stress equation for fatigue crack growth. Int. J. Frac. 24, R131-R135, 1984.
5. Dowling NE. *J*-integral estimates for cracks in infinite bodies. Eng. Frac. Mech. 226, 333-348, 1987.
6. Lehr E. Oberflächenempfindlichkeit und innere Arbeitsaufnahme der Werkstoffe bei Schwingbeanspruchung. Z. Metallkunde, 20, 78-84, 1928.
7. Siebel E, Gaier M. Untersuchungen über den Einfluß der Oberflächenbeschaffenheit auf die Dauerschwingfestigkeit metal. Bauteile bei Raumtemperatur. VDI-Z, 98, 1715-1723, 1957.
8. Hück M, Thrainer L, Schütz W. Berechnung von Wöhlerlinien für Bauteile aus Stahl, Stahlguß und Grauguß – Synthetische Wöhlerlinien. Bericht ABF11, VDEh, 1981.
9. Boller C, Seeger T. Materials data for cyclic loading. Part A – E. Elsevier, 1987.
10. Bäumel A jr. Experimentelle und numerische Untersuchung der Schwingfestigkeit randschichtverfestigter eigenspannungsbehafteter Bauteile. Ph.D. Thesis, Institut für Stahlbau und Werkstoffmechanik, Heft 49, TH Darmstadt, 1991.
11. Ramberg W, Osgood WR. Description of stress-strain curves by three parameters. Technical Report No 902, NACA, 1943.
12. Manson SS. Fatigue: A complex subject – some simple approximations. Experimental Mechanics. 5, 193-226, 1965.
13. Coffin LF jr. A study of the effects of cyclic thermal stresses on a ductile metal. Transactions of ASME, 1954:76:931-950.
14. Savaidis G, Savaidis A, Tsamasphyros G., Zhang Ch. On Size and Technological Effects in Fatigue Analysis and Prediction of Engineering Materials and Components, Int. J. Mech. Sciences, 44, 521-543, 2002.
15. Smith KN, Watson P, Topper TH. A stress-strain function for the fatigue of materials. J. of Materials, 5, 767-778, 1970.